Science and Technology Publishing (SCI & TECH)
ISSN: 2632-1017
Vol. 7 Issue 8, August - 2023

Applications of Bioinspiration in Additive Manufacturing

Joseph Long
Engineering Technology – School of Industrial Sciences and Technology
University of Central Missouri, Warrensburg Missouri, United States
jdlong@ucmo.edu

***Abstract*—Currently additive manufacturing (AM) is still primarily used for prototyping and modeling. However, with the increase in available materials and more advanced machines, AM is becoming a production process in which ready-to-ship products are being manufactured, therefore it is important to effectively use the material in AM machines. One way this can be accomplished is by modifying the infill structure that is used. This proceeding reports the on the testing and statistical analysis of the compressive strength of chopped carbon fiber reinforced nylon specimens manufactured on an Ultimaker 2+ 3D printer. Using the honeycomb, truss, and gyroid designs are examples of bioinspiration, or the use of design in nature for solving engineering problems.**

Keywords—bioinspiration,additive manufacturing, technology management, 3d printing, rapid prototyping, compressive modulus of elasticity, compressive proportional limit, maximum compressive stress

I. INTRODUCTION

Solving problems is an everyday occurrence. Problems happen, effective technology management professionals can solve them. When an exoskeleton is too heavy for a patient to even benefit from, additive manufacturing (AM) can be used to help solve this problem through bioinspiration using lightweight infill patterns and densities without compromising strength.

A. Additive Manufacturing

In the 1980s, several researchers were exploring new ways of producing parts through AM, which is officially defined as the "process of joining materials to make parts from 3D model data, usually layer upon layer, as opposed to subtractive manufacturing and formative manufacturing methodologies" [1]. Some of the potential advantages of AM that the French 3D printing company Sculpteo [2] names are: the ability to manufacture complex designs not possible through subtractive manufacturing, produce less waste material, improve designs before making costly tooling, and integrating conformal cooling channels more efficiently. Additionally, Bikas, Stavropoulos, and Chryssolouris [3] discuss the increased "design freedom" that AM offers by allowing engineers to redesign multi-part assemblies into one or two parts. Some of the industries that are using AM technology are the automotive, medical, and aerospace, to name a few. One reason for its use in the medical field is its high level of customization; take for instance dental implants, where a dental professional can 3D scan a patient's jaw and produce an implant that will fit perfectly.

In AM, objects are generally not printed as a solid object, they are made up of a shell with an internal latticework, referred to as infill, which is selected by the user and often has a pattern that is optimized to shorten print time and/or lightweight the part, while maintaining structural integrity [4]. Furthermore, Chacóna, Caminerob, García-Plazab, and Núñezb [5] explain that the printing parameters, two of which are the infill density and pattern, have a significant effect on the quality and strength of 3D printed objects. This research tested the hypothesis that bioinspired infill designs are more efficient, meaning that they have a higher compressive modulus of elasticity, compressive proportional limit, and maximum compressive stress at equal density, than a standard grid infill design.

B. Bioinspiration

> Although human genius through various inventions makes instruments corresponding to the same ends, it will never discover an invention more beautiful, nor more ready nor more economical than does nature, because in her inventions nothing is lacking, and nothing is superfluous.

These are the words of Leonardo da Vinci back in the early 1500s [6]. Da Vinci recognized that design is all around us in the natural world. Biomimicry is defined as the technical emulation of biological forms, processes, patterns, and systems [7]; other terms that are used (often interchangeably) are bioinspiration, and biomimetics. Wegst, Bai, Saiz, Tomsia, and Ritchie [8] further explain that, "today, scientists and engineers continue to be fascinated by the distinctive qualities of the elegant and complex architectures of natural structures."

One of the inspirations that has come from the living world is the honeycomb design. This multicellular hexagonal configuration is a very effective design and has been heralded as the most efficient shape to fill a two-dimensional shape plane since at least around 36 BC when Marcus Terentius Varro

wrote about the hexagonal shape of the bee's honeycomb [9]. Furthermore, Chamberland [10] commented that:

> A mathematical rational was given by the Polish polymath Jan Brożek (1585–1652): The hexagon tiles the plane with minimal boundary. Stated another way, Brożek conjectured that the optimal way to cover a large region with shapes of the same area while minimizing the boundary is to use the hexagonal structure.

The boundary that Brożek is referring to is the waxy perimeter of the structure, indicating that a honeycomb made of squares, for example, would take more wax than one made of hexagons. Hales [11] was able to mathematically demonstrate the truthfulness of the Honeycomb Conjecture. Today the honeycomb is a widely used design with many applications, from the airfoils of planes to mattresses, and even packaging.

Another design that has been inspired from the living world is the truss system which can be found in the bones of birds, among other places. Novitskaya et al. [12] report that the internal structure of many avian wings contains reinforcing structures called struts and ridges. Struts are the members that stretch across the internal walls of the bone while the ridges lie against the bone's wall. The results of these added structures are at least twofold: first, their bones are able to withstand the forces experienced in takeoff, flight, and landing, and second, maintaining a lightweight ratio. Often, the stresses experienced in the bird's bones are in the form of bending and torsion. It is believed that these reinforcing structures develop in response to the specific stresses experienced by the birds in takeoff, flight, and landing.

Novitskaya et al. [12] scanned a condor femur and a turkey vulture humerus bone utilizing a micro-computed tomography scanner to analyze the internal structure. The research team then modeled, and 3D printed (in ABS material) hollow cylindrical tubes with struts along part of the interior wall to simulate the bird bone structure. Three samples were torsion tested on an Instron 3367 Dual Column Testing System, while three others were compression tested to test the effect of the ridges on ovalization. The results of the strength testing suggested that the struts had a noticeable effect on the ovalization or compressive strength, while the results of the torsion samples did not show a noticeable effect from the struts on the torsion forces.

The final bioinspired design to be considered in this proceeding is the gyroid. NASA scientist A. Shoen was the first to describe this structure in 1970 [13]. Schoen [14] stated that the gyroid structure "contains neither straight lines nor plane lines of curvature. Thus, its symmetry group includes no mirror reflections, and the axes of rotational symmetry do not lie in the surface." Gan, Turner, and Gu [15] describe gyroids as "chiral periodic structures with a cubic symmetry." A chiral structure is one which is not superimposable on its mirror image [16] and cubic symmetry refers to the geometric nature the unit cell of the gyroid (see Fig. 1-3).

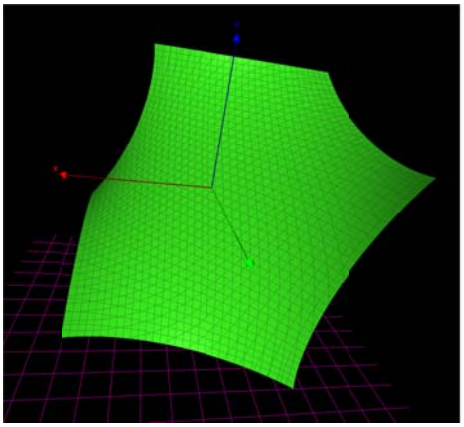

Fig. 1. *Gyroid. Single period of the gyroid structure as derived from the formula cos(x)*sin(y)+cos(y)*sin(z)+cos(z)*sin(x).*

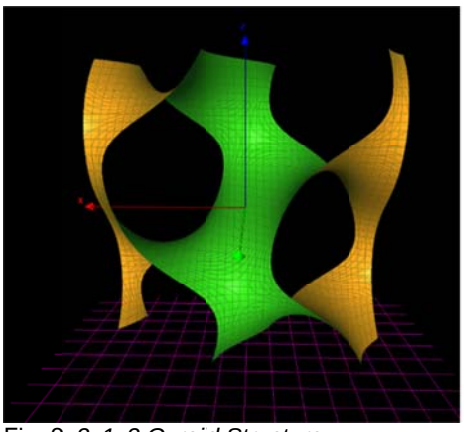

Fig. 2. *3x1x3 Gyroid Structure.*

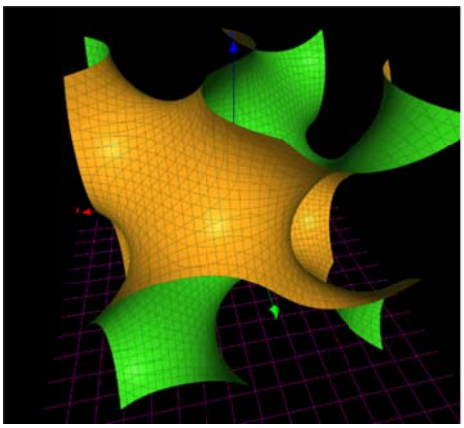

Fig. 3. *3x3x3 Gyroid Structure.*

The gyroid structure can be found in living and non-living systems. One example can be found in the wings of some species of butterflies. In the field of photonics and optics, researchers Gan, Turner, and Gu, [15] used scanning electron microscopy to study the gyroid nano-structures found in the blue-green colored wings of the *Callophrys rubi* butterfly. Similarly, Goi, Cumming, and Gu, [17] in their research described the

butterfly wing as a natural gyroid with "two unequal sub-volumes, the largest filled with air and the smallest filled with cuticle." These air and cuticle filled structures are called biophotonic nanostructures and produce the iridescent structural colors that are seen on the butterfly's wings [18,19]. The "reflectance spectrum is determined by submicrometre structural variations causing interference, diffraction or scattering creating structural, physical colors" [20].

II. Methodology

A. Design of Experiment and Data Collection

A 2 x 4 independent factorial design was used to test the hypotheses for this quantitative experimental research project (see Fig. 4). Field [21] states that this design is used when "there are several independent variables or predictors and each has been measured using different entities (between groups)."

B. Variables and Data Recording Information

A 2 x 4 independent Factorial ANOVA was used to test the hypotheses. Table 1, shows the variables that were used in the statistical analysis. It contains two nominal dichotomous independent variables, and three nominal continuous dependent variables (measured in N/mm2). The two independent variables are infill design and infill density. The dependent variables are the compressive modulus of elasticity, the compressive proportional limit, and the maximum compressive stress; these three dependent variables were calculated from the same data output that was produced in the compression testing of each specimen. The two factors and levels can be seen in Table 2.

Fig. 5 and 6 show the test specimens, with walls and top layers removed, in order to show the infill designs and infill densities. The 3D Truss infill design is not a standard infill design and thus was developed in 3DXpert for SolidWorks 14.0, see Fig. 6.

Two sets of ten test specimens and one set of five of each infill design and density were printed at a time, e.g., prints of ten and five A1s, A2s, B1s, B2s, and etcetera. A total of 200 test specimens were printed, 25 of each infill and density combination: 25 – A1s, 25 – A2s, 25 – B1s, 25 – B2s, 25 – C1s, 25 – C2s, 25 – D1s, and 25 – D2s. Fig. 8 show an example of build plates with ten and five specimens; the finished test specimens were each affixed with barcode labels for tracking purposes. As previously stated, an Ultimaker 2+ was used to print all 200 test specimens (see Fig. 7).

III. Discussion of the Results

A. Strength Comparison by Infill Design and Density

The following data, in Fig. 9 and 10, is a general comparison showing the mean compressive modulus of elasticity, compressive proportional limit, and maximum compressive stress across the tested infill densities and infill designs. A visual observation of Fig. 9 (Image a) suggests that if the compressive modulus of elasticity is of primary concern for a given part to be produced by AM, the 2D Grid infill design might be the first choice for the technology management professional at 30% or 50% infill density, followed by the 2D Honeycomb design, then the 3D Truss design, and lastly the 3D Gyroid design (if one is only selecting from the four designs used in this study). If the compressive proportional limit is of primary concern for a given part to be produced by AM, the data shown in Fig. 9 (Image b) suggests that the 2D Grid infill design might be the first choice for the technology management professional, followed by the 2D Honeycomb design, then the 3D Gyroid design, and lastly, the 3D Truss design (if one is only selecting from the four designs used in this study).

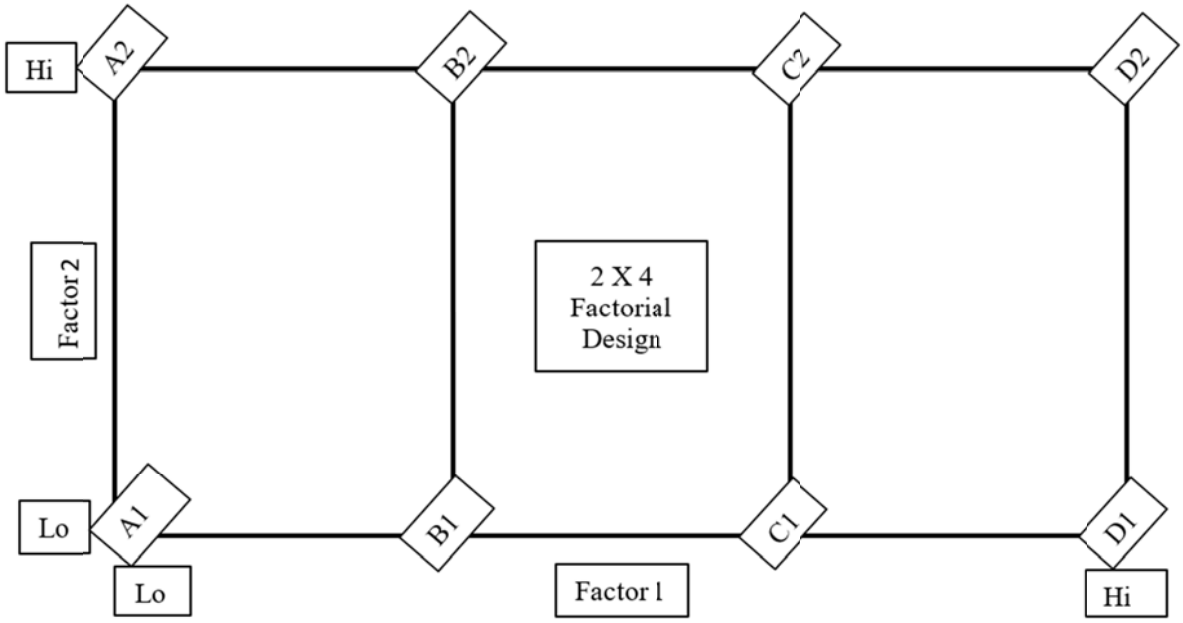

Fig. 4. *Group Divisions.*

TABLE 1. VARIABLE

	Independent / Dependent Variable	*Level of Measurement*	*Characteristics of Measurement*	*Levels*
Infill design	IV	Nominal	Dichotomous	1 = 2D Grid 2 = 2D Honeycomb 3 = 3D Truss 4 = 3D Gyroid
Infill Density	IV	Nominal	Dichotomous	1 = 30% Density 2 = 50% Density
Compressive Modulus of Elasticity (N/mm^2)	DV	Ratio	Continuous	(N/mm^2)
Compressive Proportional Limit (N/mm^2)	DV	Ratio	Continuous	(N/mm^2)
Maximum Compressive Stress (N/mm^2)	DV	Ratio	Continuous	(N/mm^2)

TABLE 2. GROUP DIVISIONS

Group	*Factor 1*	*Factor 2*
A1	2D Grid	30% Density
B1	2D Honeycomb	30% Density
C1	3D Truss	30% Density
D1	3D Gyroid	30% Density
A2	2D Grid	50% Density
B2	2D Honeycomb	50% Density
C2	3D Truss	50% Density
D2	3D Gyroid	50% Density

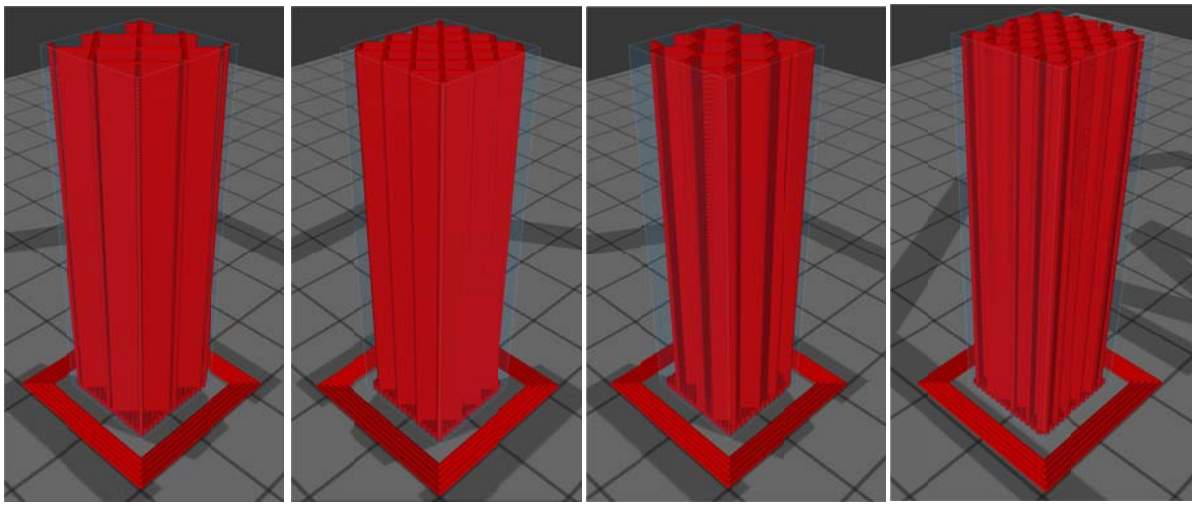

Fig. 5. *3D Representation of Test Specimen. The difference in a 30% and 50% infill density can be seen in the images above (a) is the 2DGrid design at 30% density, (b) is the 2DGrid design at 50% density, (c) is the 2DHoneycomb at 30% density, and (d) is the 2DHoneycomb at 50% density.*

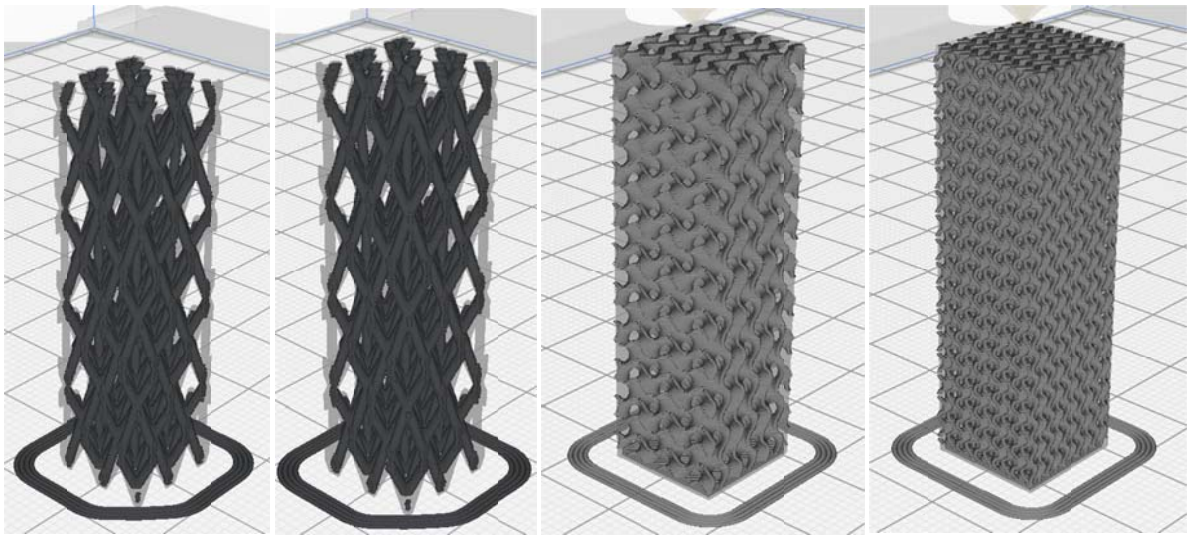

Fig. 6. *3D Representation of Test Specimen. The difference in a 30% and 50% infill density can be seen in the images above (a) is the 3DTruss design at 30% density, (b) is the 3DTruss design at 50% density, (c) is the 3DGyroid at 30% density, and (d) is the 3Dgyroid at 50% density.*

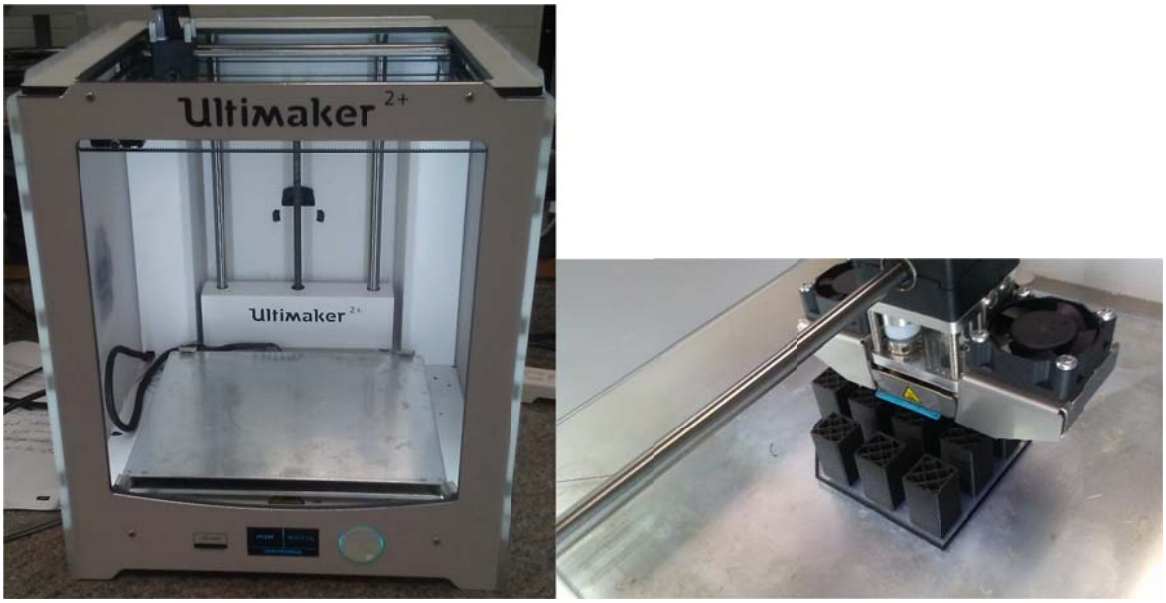

a b

Fig. 7. *Ultimaker and Printing. Image (a) shows the 3D printer used to produce the 200-test specimen. Image (b) shows the Ultimaker building ten of the A1 prints.*

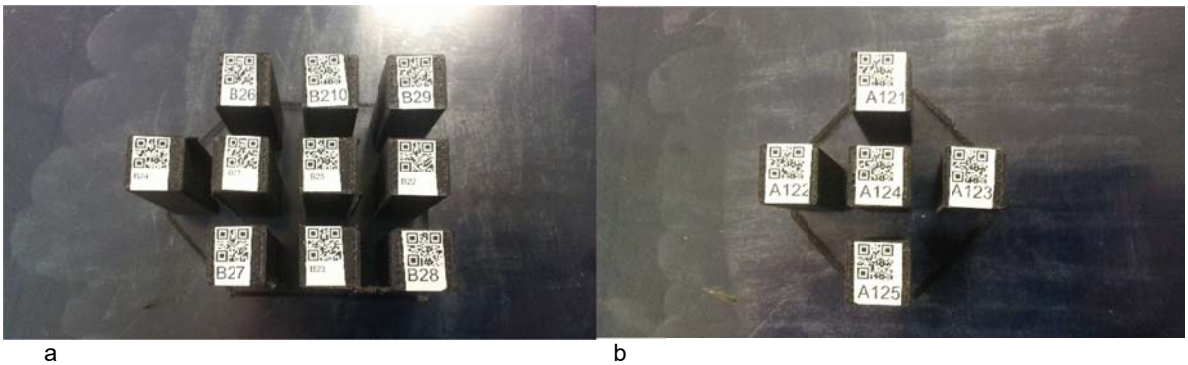

a b

Fig. 8. *Example of Build Plates. Test specimen were built in batches of ten (a) and five (b).*

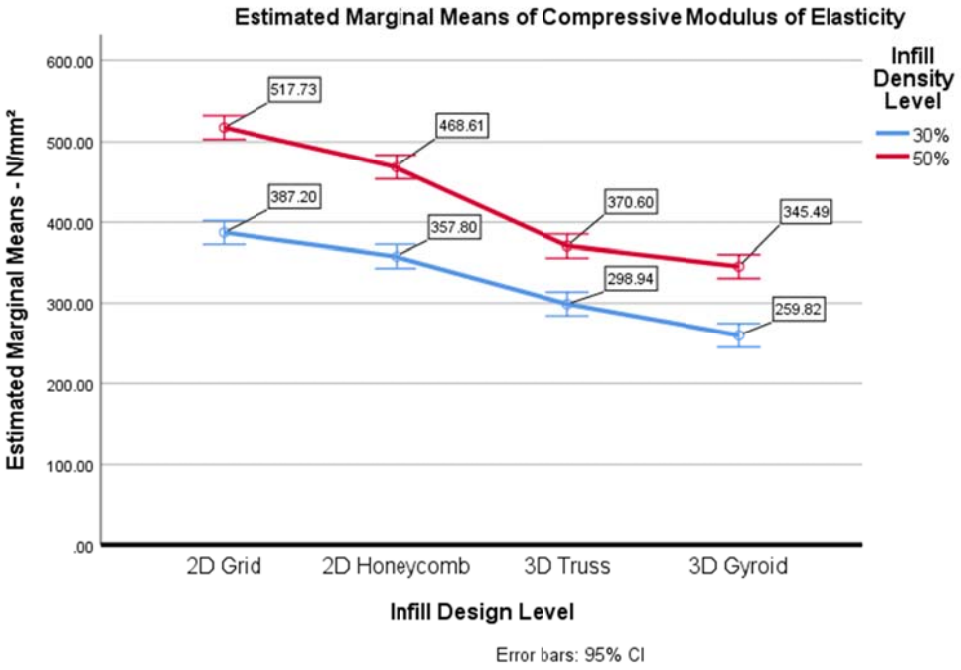

a

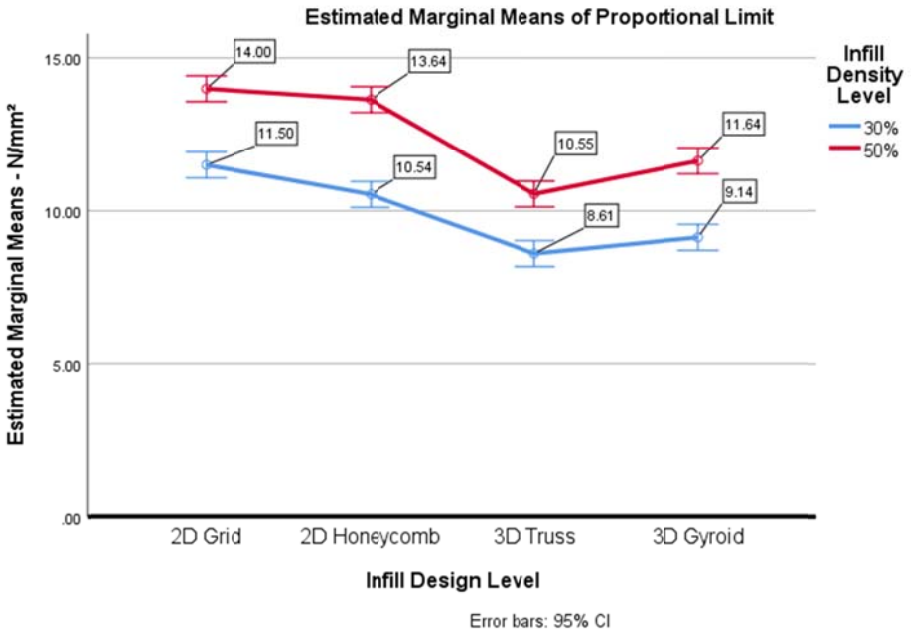

b

Fig. 9. *Estimated Marginal Means. Image (a) displays a plot of the data collected during the study for the compressive modulus of elasticity, while image (b) displays that of the compressive proportional limit.*

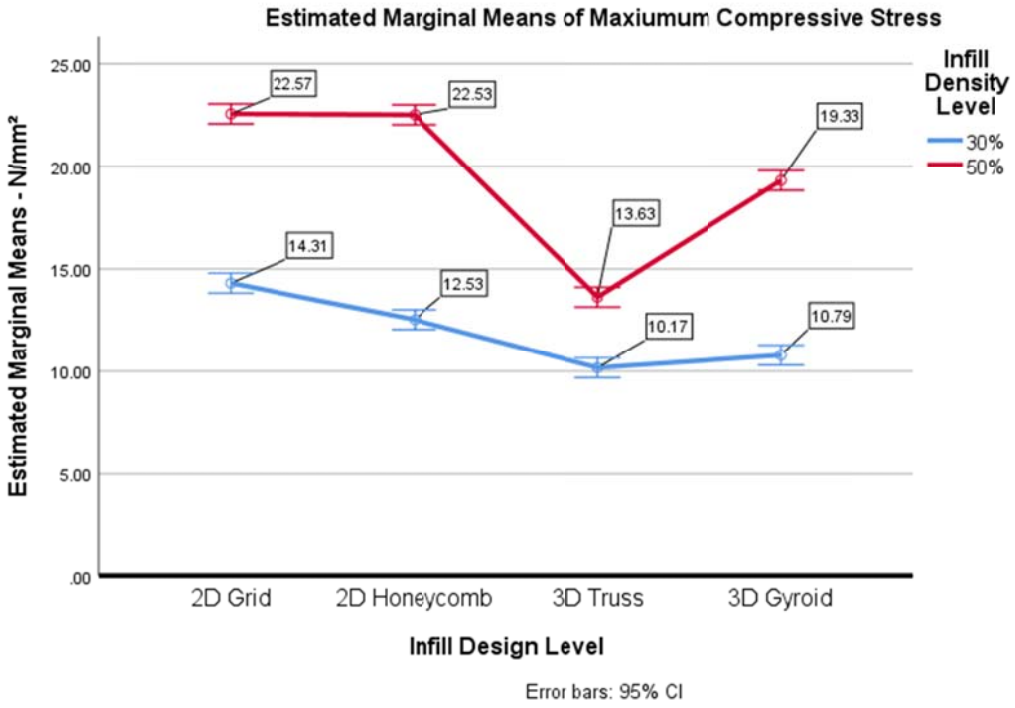

Fig. 10. *Estimated Marginal Means. This figure displays a plot of the data collected during the study for the maximum compressive stress.*

And finally, if the maximum compressive stress is the primary concern for a given part to be produced by AM, the data shown in Fig. 10 suggests that the 2D Grid and the 2D Honeycomb infill designs are nearly equal (at 50% density) implying that either one may be a good first choice for the technology management professional, followed by the 3D Gyroid design, and lastly, the 3D Truss design (if one is only selecting from the four designs used in this study).

As demonstrated in the results of this research, there is a statistically significant difference in the compressive modulus of elasticity, the compressive proportional limit, and the maximum compressive stress between levels for the infill density and infill designs. These significant differences indicate that technology management professionals should be careful when choosing an infill density and an infill design for a part to be produced by AM when the compressive modulus of elasticity, compressive proportional limit, and maximum compressive stress is a concern.

B. Practical Implications and Applications

Consequently, some practical implications of this research are the possibility that the selection of various levels of infill density and infill deign used to produce a given part through AM would result in a significantly higher or lower compressive modulus of elasticity, compressive proportional limit, or maximum compressive stress. For technology management professionals conducting research in the field of AM, these results imply that further research will be necessary to determine the amount of variation assignable to infill density and infill design, as it effects the compressive modulus of elasticity, compressive proportional limit, or maximum compressive stress.

The interactions of 30% x 2Dgrid, 50% x 2Dgrid, 30% x 2Dhoneycomb, 50% x 2Dhoneycomb, 30% x 3Dtruss, 50% x 3Dtruss, 30% x 3Dgyroid, and 50% x 3Dgyroid all show differences in compressive modulus of elasticity, compressive proportional limit, or maximum compressive stress results. Hence, despite a lack of statistical difference in the compressive proportional limit, based on the combined infill designs and infill densities, the results will be a difference in the compressive proportional limit.

To include examples of research that validates the findings of the current research, Brischetto, Ferro, Maggiore, & Torre [22] yielded the following averages for their ABS specimens:

- Compressive modulus of elasticity of 805.1 N/mm²
- Compressive proportional limit of 28.49 N/mm²
- Maximum compressive stress of 37.51 N/mm²

Although their results are higher than those of the current study (see Fig. 9 & 10), this is likely due to the internal nature of the specimens as Brischetto, Ferro, Maggiore, & Torre [22] tested 100% solid specimens.

The results of this study have demonstrated that the selected infill design and infill density will result in a significant amount of variation when they are changed by the technology management professional. This illustrates the necessity of the technology management professional's ability to conduct research and develop

strategies and plans to identify, develop, and implement innovative AM-based solutions.

The implications of these results are important to technology management professionals, and users of AM equipment for hobby, prototyping, production, or research. As previously discussed, one of the great advantages of AM is that users can easily change the infill density and infill design of parts to be produced. In the automotive and aerospace fields for instance, light weighting of parts is of great concern for fuel efficiency. Moreover, with the rise of more costly materials such as carbon fiber and metals, the choice of infill design and infill density can have a very pricy impact on the part to be produced.

Returning to the scenario in the introduction of an exoskeleton that is too heavy for a patient to even benefit from, consider the following study of an exoskeleton being designed and developed for an infant. Babik et al. [23] tested the feasibility and effectiveness of an exoskeleton for improving the arm movements of an 8-month-old with arthrogryposis (a disorder where infants are born with significant muscle contractures and weakness across multiple joints). The exoskeleton that was used in the study was produced with AM equipment, using strong but lightweight polymer material, making it very helpful to the infant. Tools such as these can assist with play and movement in young infants during this very crucial developmental phase. Two crucial variables that a technology management professional must set for producing products, such as exoskeletons, on AM equipment are infill density and infill design. Hopefully, this study will be welcomed as a unique combination of infill designs, infill densities, and their effect on the compressive modulus of elasticity, compressive proportional limit, and maximum compressive stress of parts produced with NylonX polymer material.

REFERENCES

[1] ISO/ASTM52900 – 15. "Standard Terminology for Additive Manufacturing — General Principles — Terminology1". ASTM International, West Conshohocken, PA, 2015. Available online: www.astm.org (accessed on 16 July 2017).

[2] Sculpteo. (2017). The complete metal 3D printing guide. Retrieved from https://www.sculpteo.com/en/get/ebook/the-complete-metal-3d-printing-guide/.

[3] Bikas, H., Stavropoulos, P., & Chryssolouris, G. (2016). Additive manufacturing methods and modelling approaches: A critical review. *The International Journal of Advanced Manufacturing Technology*, vol. 83, no. 1, pp. 389-405. doi:10.1007/s00170-015-7576-2.

[4] Wu, J., Aage, N., Westermann, R., & Sigmund, O. (2017). Infill optimization for additive manufacturing-approaching bone-like porous ptructures. *IEEE Transactions on Visualization and Computer Graphics*.

[5] Chacón, J., Caminero, M., García-Plaza, E., & Núñez, P. (2017). Additive manufacturing of PLA structures using fused deposition modelling: Effect of process parameters on mechanical properties and their optimal selection. *Materials & Design*, vol. 124, pp. 143-157. doi:10.1016/j.matdes.2017.03.065.

[6] Thompson, B. S. (1999). Environmentally-sensitive design: Leonardo WAS right!. *Materials & Design*, vol. 20, no. 1, pp. 23-30.

[7] Benyus, J. M. (2013). A biomimicry primer. Retrieved from https://biomimicry.net/b38files/A_Biomimicry_Primer_Janine_Benyus.pdf.

[8] Wegst, U. G. K., Bai, H., Saiz, E., Tomsia, A. P., & Ritchie, R. O. (2015). Bioinspired structural materials. *Nature Materials*, vol. 14, no. 1, pp. 23-36. doi:http://dx.doi.org/10.1038/nmat4089.

[9] Hales, T. C. (2002). The honeycomb conjecture. Retrieved from https://arxiv.org/pdf/math/9906042.pdf.

[10] Chamberland, M. (2015). Single digits: In praise of small numbers. Princeton: Princeton University Press, p. 57.

[11] Hales, T. C. (2002). The honeycomb conjecture. Retrieved from https://arxiv.org/pdf/math/9906042.pdf.

[12] Novitskaya, E., Ruestes, C. J., Porter, M. M., Lubarda, V. A., Meyers, M. A., & McKittrick, J. (2017). Reinforcements in avian wing bones: Experiments, analysis, and modeling. *Journal of the Mechanical Behavior of Biomedical Materials,* vol. 76, no. 85.

[13] Podroužek, J., Marcon, M., Ninčević, K., & Wan-Wendner, R. (2019). Bio-Inspired 3D Infill Patterns for Additive Manufacturing and Structural Applications. *Materials (Basel, Switzerland)*, vol. 12, no. 3, p. 499. doi:10.3390/ma12030499.

[14] Schoen, A. (1970). *Infinite Periodic Minimal Surfaces Without Self-Intersections - NASA-TN-D-5541*. Retrieved from http://hdl.handle.net/2060/19700020472.

[15] Gan, Z., Turner, M., & Gu, M. (2016). Biomimetic gyroid nanostructures exceeding their natural origins. *Science Advances*, vol. 2, no. 5, e1600084. https://doi.org/10.1126/sciadv.1600084.

[16] Khan Academy (producer). (2019). Introduction to chirality (video). Accessed June 26, 2019. https://www.khanacademy.org/science/organic-chemistry/stereochemistry-topic/chirality-r-s-system/v/introduction-to-chirality.

[17] Goi, E., Cumming, B. P., & Gu, M. (2018). Gyroid "srs" networks: Photonic materials beyond

nature. *Advanced Optical Materials,* vol. 6, no. 18, 1800485-n/a. doi:10.1002/adom.201800485.

[18] Saranathan, V., Osuji, C. O., Mochrie, S. G. J., Noh, H., Narayanan, S., Sandy, A., Dufresne, E. R., Prum, R. O. (2010). Structure, function, and self-assembly of single network gyroid ($I4_132$) photonic crystals in butterfly wing scales. *Proceedings of the National Academy of Sciences,* vol. 107, no. 26 11676-11681; DOI:10.1073/pnas.0909616107.

[19] Pouya, C. , Overvelde, J. T., Kolle, M. , Aizenberg, J. , Bertoldi, K. , Weaver, J. C. and Vukusic, P. (2016), Characterization of a Mechanically Tunable Gyroid Photonic Crystal Inspired by the Butterfly *Parides Sesostris*. *Advanced Optical Materials,* vol. 4, pp. 99-105. doi:10.1002/adom.201500436.

[20] Michielsen, K., & Stavenga, D. G. (2008). Gyroid cuticular structures in butterfly wing scales: Biological photonic crystals. *Journal of the Royal Society, Interface,* vol. 5, no. 18, p. 85.

[21] Field, A. P. (2018). *Discovering Statistics Using SPSS.* 5th ed. Los Angeles. Thousand Oaks, Calif.: SAGE Publications.

[22] Chacón, J., Caminero, M., García-Plaza, E., & Núñez, P. (2017). Additive manufacturing of PLA structures using fused deposition modelling: Effect of process parameters on mechanical properties and their optimal selection. *Materials & Design,* vol. 124, pp. 143-157. doi:10.1016/j.matdes.2017.03.065.

[23] Babik, I., Kokkoni, E., Cunha, A. B., Galloway, J. C., Rahman, T., & Lobo, M. A. (2016). Feasibility and effectiveness of a novel exoskeleton for an infant with arm movement impairments. *Pediatric Physical Therapy: The Official Publication of the Section on Pediatrics of the American Physical Therapy Association*, vol. 28, no. 3, p. 338.